Supporting Information

Light–Driven, Proton–Controlled, Catalytic Aerobic C–H Oxidation Mediated by a Mn(III) Porphyrinoid Complex

Heather M. Neu,[†] Jieun Jung,[‖] Regina A. Baglia,[†] Maxime A. Siegler,[†] Kei Ohkubo,[‖] Shunichi Fukuzumi,[*,‖,‡] and David P. Goldberg[*,†]

[†]Department of Chemistry, The Johns Hopkins University, Baltimore, Maryland 21218, United States

[‖] Department of Material and Life Science, Graduate School of Engineering, Osaka University, ALCA, Japan Science and Technology Agency, Suita, Osaka 565-0871, Japan

[‡]Department of Bioinspired Science, Ewha Womans University, Seoul 120–750, Korea

E-mail: dpg@jhu.edu, fukuzumi@chem.eng.osaka-u.ac.jp

Materials. All reactions were performed using dry solvents and standard Schlenk line techniques unless noted otherwise. The $Mn^{III}(TBP_8Cz)$ and $Mn^{V}(O)(TBP_8Cz)$ complexes (TBP_8Cz = octakis(*p–tert–*butylphenyl)corrolazinato^{3-}) were synthesized according to previously published methods.[1] The oxonium acid, $[H(OEt_2)_2]^+[B(C_6F_5)_4]^-$ was prepared according to published procedures.[2] Solvents were purified via a Pure–Solv solvent purification system from Innovative Technologies, Inc. Deuterated solvents used for NMR samples were purchased from Cambridge Isotope Laboratories, Inc. All other reagents were purchased from Sigma–Aldrich at the highest level of purity and were used as received.

Instrumentation. UV–vis spectroscopy and other UV–vis measurements were performed on a Hewlett–Packard 8453 diode–array spectrophotometer equipped with HP Chemstation software. A 400 nm longpass filter was employed to prevent decomposition of $[Mn^{III}(H_2O)(TBP_8Cz(H))][B(C_6F_5)_4]$ or $[Mn^{III}(H_2O)(TBP_8Cz(H)_2)][B(C_6F_5)_4]_2$ by placing the filter directly between the sample quartz cuvette and the spectrophotometer light source to block UV–light. For catalysis experiments, the sample was irradiated by a Cole–Parmer Illuminator equipped with a halogen lamp (150 W). The low temperature UV–vis measurements were performed on a Hewlett Packard 8453 diode–array spectrophotometer equipped with an Unisoku USP–203A cryostat, using a 1 cm modified Schlenk cuvette. Gas chromatography (GC) was carried out on an Agilent 6850 gas chromatograph fitted with a DB–5 5% phenylmethyl siloxane capillary column (30 m x 0.32 mm x 0.25 μm) and equipped with a flame–ionization detector. Elemental analyses were performed at Atlantic Microlab, Inc., Norcross, GA. The NMR experiments were measured on a Bruker 300 MHz spectrometer and chemical shifts are reported in parts per million against the residual solvent signal.

Catalytic Reactions. For the catalytic reactions where the catalyst was generated in situ, $[H(OEt_2)_2]^+[B(C_6F_5)_4]^-$ ($H^+[B(C_6F_5)_4]^-$) (32 μM) and hexamethylbenzene (16 mM) were added to a solution of $Mn^{III}(H_2O)(TBP_8Cz)$ (16 μM) in benzene (2 mL) at 23 °C. When crystalline material was used as catalyst, HMB (27 mM) was added to a solution of $[Mn^{III}(H_2O)(TBP_8Cz(H)_2)][B(C_6F_5)_4]_2$ (27 μM) in benzene (3 mL) at 23 °C. For both types of reactions, the solution was then transferred to a cuvette equipped with a stir bar. The reaction was then irradiated with visible ($\lambda > 400$ nm) light with stirring under aerobic conditions. The reaction was monitored by UV–vis and showed a rapid conversion of diprotonated $[Mn^{III}(H_2O)(TBP_8Cz(H)_2)][B(C_6F_5)_4]_2$ (λ_{max}: 470, 763 nm) to monoprotonated

$[Mn^{III}(H_2O)(TBP_8Cz(H))][B(C_6F_5)_4]$ (446, 728 nm), and then a slow bleaching of the two bands at 446 and 728 nm. During the reaction, aliquots of the reaction mixture were removed, dodecane was added as an internal standard, and the solution was analyzed by GC–FID. The products, pentamethylbenzyl alcohol and pentamethylbenzaldehyde, were identified by comparison with a standard sample. Yields were obtained by comparing the integration of the product peak with the integration of the internal standard peak.

Photoirradiation of crystalline $[Mn^{III}(H_2O)(TBP_8Cz(H))]^+$ with HMB under aerobic conditions. A solution of $[Mn^{III}(H_2O)(TBP_8Cz(H))][B(C_6F_5)_4]$ (22 μM) in CH_2Cl_2 (2 mL) was loaded into a quartz cuvette (1 cm path length). The cuvette was then clamped inside the UV–vis spectrophotometer so that spectra could be collected during photoirradiation. A Cole–Parmer Illuminator equipped with a halogen lamp (150 W) was positioned at a distance of 15 cm from the quartz cuvette ~90° to the UV–vis beam. A 400 nm long–pass filter was placed between the cuvette and the lamp and another 400 nm long–pass filter placed between the cuvette and the spectrophotometer light source. To initiate the reaction, hexamethylbenzene (22 mM) was added to the cuvette and the solution was irradiated under aerobic conditions. The changes in absorbance were monitored by UV − vis spectroscopy showing the isosbestic decay of $[Mn^{III}(H_2O)(TBP_8Cz(H))][B(C_6F_5)_4]$ (λ_{max} = 446, 730 nm) and formation of $[Mn^{IV}(O)(TBP_8Cz^{+\bullet})(H)]^+$ (λ_{max} = 418, 784 nm). Products were analyzed by GC–FID.

Crystallization of $Mn^{III}(H_2O)(TBP_8Cz)$. To a solution of $Mn^{V}(O)(TBP_8Cz)$ (2 μmol) in CH_2Cl_2 (750 μL) was added 1 equiv $B(C_6F_5)_3$ (2 μmol). A color change from green to brown was observed. An amount of acetonitrile (190 μL) was added to the reaction mixture to facilitate crystallization. The solvent mixture evaporated slowly over the course of 1.5 weeks to give large block–shaped brown crystals which were identified as the $Mn^{III}(H_2O)(TBP_8Cz)$ complex by X–ray diffraction.

Synthesis of $[Mn^{III}(H_2O)(TBP_8Cz(H))][B(C_6F_5)_4]$. To a solution of $Mn^{III}(H_2O)(TBP_8Cz)$ (6 mM) was added $H^+[B(C_6F_5)_4]^-$ (6 mM) in CH_2Cl_2 (1 mL). The UV–vis spectrum of the reaction mixture after $H^+[B(C_6F_5)_4]^-$ addition showed two strong bands (λ_{max}: 446, 730 nm). This reaction mixture was then concentrated to dryness and redissolved in toluene (1 mL). The toluene solution was divided between five NMR tubes and layered with n–heptane. X–ray quality, dark brown block crystals were obtained after 4 d. UV–vis (CH_2Cl_2): λ_{max}, nm ($\varepsilon \times 10^{-4}$ M^{-1} cm^{-1}) = 446 (6.08), 730 (3.09). UV–vis (benzene): λ_{max}, nm ($\varepsilon \times 10^{-4}$ M^{-1} cm^{-1}) = 446 (6.00),

728 (3.06). Anal. Calcd for $C_{120}H_{107}BF_{20}MnN_7O$: C, 68.34; H, 5.11; N, 4.65. Found: C, 68.23; H, 5.17; N, 4.66.

Synthesis of $[Mn^{III}(H_2O)(TBP_8Cz(H)_2)][B(C_6F_5)_4]_2$. To a solution of $Mn^{III}(H_2O)(TBP_8Cz)$ (3 mM) was added two equivalents of $H^+[B(C_6F_5)_4]^-$ (6 mM) in CH_2Cl_2 (0.5 mL). The UV–vis spectrum of the reaction mixture showed two bands (λ_{max}: 470, 763 nm). The reaction mixture was then concentrated to dryness and redissolved in toluene (500 μL). The toluene solution was transferred to a NMR tube and layered with n–heptane. X–ray quality, dark brown thick lath crystals were obtained after one week. UV–vis (CH_2Cl_2): λ_{max}, nm ($\varepsilon \times 10^{-4}$ M^{-1} cm^{-1}) = 470 (5.03), 763 (2.82). Anal. Calcd for $C_{144}H_{108}B_2F_{40}MnN_7O$: C, 62.01; H, 3.90; N, 3.52. Found: C, 62.43; H, 4.32; N, 3.31.

Low temperature reaction of $Mn^V(O)(TBP_8Cz)$ with $H^+[B(C_6F_5)_4]^-$ and 1,8–bis(dimethylamino)naphthalene (proton sponge). A solution of $Mn^V(O)(TBP_8Cz)$ (19 μM) in CH_2Cl_2 (3 mL) was cooled to –60 °C. The reaction was then initiated by the addition of $H^+[B(C_6F_5)_4]^-$ (19 μM) and the temperature was maintained at –60 ±0.1°C throughout the reaction. The changes in absorbance were monitored by UV–vis spectroscopy showing the isosbestic decay of $Mn^V(O)(TBP_8Cz)$ (λ_{max} = 419, 634 nm) and formation of $[Mn^V(O)(TBP_8Cz)(H)]^+$ (λ_{max} = 436, 650 nm). Upon addition of one equivalent of proton sponge (19 μM) the spectrum converted back to the original $Mn^V(O)(TBP_8Cz)$ spectrum (λ_{max} = 419, 634 nm) with some minor $Mn^{III}(TBP_8Cz)$ production.

Low temperature NMR studies of $[Mn^V(O)(TBP_8Cz)(H)]^+$. A solution of $Mn^V(O)(TBP_8Cz)$ (1 mM for ^{1}H–NMR and 3.9 mM for ^{1}H–^{1}H COSY and ^{1}H–^{1}H NOESY experiments) in CD_2Cl_2 (400 μL) was transferred to an NMR tube and cooled to –60 °C. Upon addition of one equivalent of $H^+[B(C_6F_5)_4]^-$, a color change from green to dark brown was observed. This sample was kept at –60 °C and transferred to a –60 °C pre-cooled 300 MHz NMR spectrometer for analysis. ^{1}H–NMR (300 MHz, methylene chloride–d_2) δ 13.45 (s, 1H, NH), 8.40 (m, 7H, Ar), 8.04 (m, 4H, Ar), 7.87 (m, 2H, Ar), 7.81 – 7.64 (m, 9H, Ar), 7.63 – 7.46 (m, 6H, Ar), 7.21 (m, 4H, $H_{C,E}$), 1.51 – 1.44 (m, 37H, tBu), 1.41 (s, 18H, tBu), 1.30 (m, 18H, tBu).

D_2O exchange. A solution of $Mn^V(O)(TBP_8Cz)$ (1.4 mM) in CD_2Cl_2 (400 μL) was transferred to a NMR tube and cooled to –60 °C. Upon addition of one equivalent of $H^+[B(C_6F_5)_4]^-$ a color change from green to dark brown was observed, and excess D_2O (63 mM

dissolved in CD_2Cl_2) was added to the cold sample. This sample was kept at –60 °C and transferred to a –60 °C pre-cooled 300 MHz NMR for analysis.

X–ray Crystallography.

Experimental. All reflection intensities were measured at 110(2) K using a SuperNova diffractometer (equipped with Atlas detector) with Cu *K*α radiation (λ = 1.54178 Å) under the program CrysAlisPro (Versions 1.171.36.24 or 1.171.36.28 Agilent Technologies, 2012-2013). The same program was used to refine the cell dimensions and for data reduction. The structures were solved with the program SHELXS–2013[3] and were refined on F^2 with SHELXL–2013.[3] Analytical numeric absorption correction based on a multifaceted crystal model was applied using CrysAlisPro. The temperature of the data collection was controlled using the system Cryojet (manufactured by Oxford Instruments). The H atoms were placed at calculated positions (unless otherwise specified) using the instructions AFIX 23 (only for $Mn^{III}(H_2O)(TBP_8Cz)$), AFIX 43 or AFIX 137 with isotropic displacement parameters having values 1.2 or 1.5 times *U*eq of the attached C or N atoms. The H atoms of the coordinated water molecule were found from difference Fourier maps, and their coordinates were refined freely (the DFIX restraint was used to restrained the O–H bond to be 0.84(3) Å).

$Mn^{III}(H_2O)(TBP_8Cz)$: The structure is disordered. The whole corrolazine ligand is most likely disordered over two orientations. The model only includes the two disordered components of the corrolazine platform (*i.e.*, without the TBP groups) and the tert–butyl substituents of three TBP groups. As the major component of the disorder for the corrolazine platform refines to 0.824(4), it is rather difficult to locate accurately the TBP groups of the minor component. The crystal lattice also includes some amount of ordered and disordered lattice solvent molecules (DCM and acetonitrile). In the refined model, the asymmetric unit contains one ordered DCM molecule, for which its occupancy factor refines to 0.775(7), and one fully occupied ordered acetonitrile molecule. The asymmetric unit contains also some other disordered solvent molecules (DCM and acetonitrile). In the final refinement, their contributions have been taken out using the program SQUEEZE.[4] All details of the SQUEEZE refinement are provided in the final CIF file. Fw = 1535.38, irregular black plate, 0.29 × 0.24 × 0.11 mm^3, triclinic, *P*–1 (no. 2), a = 12.9561(3), b = 19.0001(4), c = 20.8656(5) Å, α = 108.1386(18), β = 98.7143(18), γ = 96.9120(16)°, V = 4747.49(19) $Å^3$, Z = 2, D_x = 1.074 g cm^{-3}, μ = 1.889 mm^{-1}, abs. corr. range: 0.653–0.876. 47685 Reflections were measured up to a resolution of $(\sin \theta/\lambda)_{max}$ = 0.59 $Å^{-1}$.

17010 Reflections were unique (R_{int} = 0.0288), of which 14916 were observed [$I > 2\sigma(I)$]. 1249 Parameters were refined using 1037 parameters. $R1/wR2$ [$I > 2\sigma(I)$]: 0.0698/0.2012. $R1/wR2$ [all refl.]: 0.0779/0.2106. S = 1.031. Residual electron density found between −0.41 and 1.01 e Å^{-3}.

Additional note: the checkCIF report contains five potential alerts level B. One alert is concerned with the rather large Ueq(max)/Ueq(min) ratio for some C atoms (t-butyl). This is not surprising as the t-butyl groups in TBP_8Cz are prone to be very disordered. Another alert suggests that one of the two H atoms of the axial water ligand does not participate in O-H...N hydrogen bonds, which is indeed correct. The three remaining B alerts can be ignored as they suggest that there is a possible missing H atoms on C33', C43' and C93', which is obviously not possible.

$[Mn^{III}(H_2O)(TBP_8Cz(H))][B(C_6F_5)_4]$: The structure is disordered. The whole corrolazine ligand is disordered over two orientations. The occupancy factor of the major component of the disorder refines to 0.7201(15). The asymmetric unit contains one Mn complex, one $B(C_6F_5)_4$ counterion, and some very disordered lattice solvent molecules (Toluene), for which their contributions had been taken out using the program SQUEEZE for the final refinement. Details of the SQUEEZE refinement are provided in the final CIF file. Fw = 2108.87, dark brown block, 0.47 × 0.36 × 0.21 mm^3, triclinic, *P*–1 (no. 2), a = 17.7599(4), b = 20.8114(5), c = 21.8473(5) Å, α = 65.375(2), β = 66.893(2), γ = 71.678(2)°, V = 6640.9(3) Å^3, Z = 2, D_x = 1.055 g cm^{-3}, μ = 1.415 mm^{-1}, abs. corr. range: 0.616–0.790. 75345 Reflections were measured up to a resolution of (sin $\theta/\lambda)_{max}$ = 0.59 Å^{-1}. 23788 Reflections were unique (R_{int} = 0.0243), of which 18815 were observed [$I > 2\sigma(I)$]. 2333 Parameters were refined using 4446 restraints. $R1/wR2$ [$I > 2\sigma(I)$]: 0.0785/0.2416. $R1/wR2$ [all refl.]: 0.0891/0.2556. S = 1.094. Residual electron density found between −0.63 and 0.87 e Å^{-3}.

Additional note: the checkCIF report contains one potential alert level B. This alert suggests that one of the two H atoms of the axial water ligand does not participate in O-H...N hydrogen bonds, which is indeed correct.

$[Mn^{III}(H_2O)(TBP_8Cz(H)_2)][B(C_6F_5)_4]_2$.: The structure is mostly ordered. The asymmetric unit contains one Mn complex, two $B(C_6F_5)_4$ counterions, and some lattice solvent molecules (toluene and possibly heptane). The Mn complex (with the corrolazine ligand) is ordered except for one *tert*–butyl group (major: C33 > C36, minor: C33' > C36'), and one *tert*–butyl phenyl group (major: C67 > C76, minor: C67' > C76'), which are both disordered over two

orientations. The occupancy factors of their major components refine to 0.798(7) and 0.790(9), respectively. All lattice toluene molecules have been successfully modeled in the final refinement; three are found to be ordered but have partial occupancies (occupancy factors: 0.662(5), 0.876(5), and 0.673(5)), and two others are found to be disordered over two orientations (major occupancy factors: 0.535(4), 0.539(10)). The asymmetric unit also includes some amount of very disordered lattice solvent molecules (possibly heptane), for which the contribution had been taken out using the program SQUEEZE for the final refinement. Details of the SQUEEZE refinement are provided in the final CIF file. Fw = 3177.40, dark brown thick lath, 0.66 × 0.33 × 0.15 mm^3, triclinic, *P*–1 (no. 2), a = 13.4086(2), b = 21.2539(3), c = 30.7514(4) Å, α = 99.0162(11), β = 93.4131(11), γ = 105.1106(14)°, V = 8309.7(2) $Å^3$, Z = 2, D_x = 1.270 g cm^{-3}, μ = 1.488 mm^{-1}, abs. corr. range: 0.542–0.841. 123818 Reflections were measured up to a resolution of $(\sin \theta/\lambda)_{max}$ = 0.62 $Å^{-1}$. 32501 Reflections were unique (R_{int} = 0.0322), of which 29309 were observed [$I > 2\sigma(I)$]. 2295 Parameters were refined using 1030 restraints. $R1/wR2$ [$I > 2\sigma(I)$]: 0.0620/0.1771. $R1/wR2$ [all refl.]: 0.0661/0.1811. S = 1.030. Residual electron density found between −0.53 and 1.06 e $Å^{-3}$.

Additional note: the checkCIF report contains two potential alerts level B. The first alert is concerned with the small average phenyl C-C bond of the toluene molecule C8S→C14S. This alert may suggest that the toluene molecule is slightly disordered. As this lattice solvent molecule is only partially occupied, no disorder model was attempted. The second alert suggests that one of the two H atoms of the axial water ligand does not participate in any hydrogen bonds, which is indeed correct.

Location of meso–N–H atoms: In the mostly ordered structure of the doubly protonated compound $[Mn^{III}(H_2O)(TBP_8Cz(H)_2)][B(C_6F_5)_4]_2$, the locations of the H atoms attached to N1 and N5 are unambiguously determined by examining the contoured difference Fourier maps in the plane defined by the atoms N1, N3 and N5 (Figure S2). In the structure of singly-protonated $[Mn^{III}(H_2O)(TBP_8Cz(H))][B(C_6F_5)_4]$, the Mn(III) corrolazine is found to be disordered over two orientations (except for Mn–OH_2), and the occupancy factor of the major component refines to *ca.* 72%. The occurrence of disorder, combined with the low scattering power of Hydrogen with X-rays, makes the search for the location of the H atom difficult. The potential N–H sites are N1, N3 or N5 for the major component of the disorder. The H atom cannot be located on N5 as this nitrogen atom is the H-bond acceptor in one intermolecular O_{water}–H…N hydrogen bond (the

location of the H atoms of the axial water ligand have been determined, see Figure S1). Hence, the H atom can only be found either on N1 or N3. One very weak residual electron density peak (0.22 e^{-} $Å^{-3}$) was observed at 1.05 Å from N1, but no residual electron density peak (even as low as 0.13 e^{-} $Å^{-3}$) could be found near N3. The doubly-protonated $[Mn^{III}(H_2O)(TBP_8Cz(H)_2)][B(C_6F_5)_4]_2$ is also not protonated on N3. In addition, our low-temp NMR data on the $Mn^{V}(O)$ complex provide strong evidence that this complex is only protonated at one of the equivalent (N1 or N5) sites. We conclude that the H atom is most likely located on N1.

References:

(1) Lansky, D. E.; Mandimutsira, B.; Ramdhanie, B.; Clausen, M.; Penner-Hahn, J.; Zvyagin, S. A.; Telser, J.; Krzystek, J.; Zhan, R. Q.; Ou, Z. P.; Kadish, K. M.; Zakharov, L.; Rheingold, A. L.; Goldberg, D. P. *Inorg. Chem.* **2005**, *44*, 4485-4498.
(2) Jutzi, P.; Muller, C.; Stammler, A.; Stammler, H. G. *Organometallics* **2000**, *19*, 1442-1444.
(3) Sheldrick, G. M. *Acta Crystallogr A* **2008**, *64*, 112-122.
(4) Spek, A. L. *J Appl Crystallogr* **2003**, *36*, 7-13.

Scheme S1. Addition of H^+ to $Mn^V(O)(TBP_8Cz)$

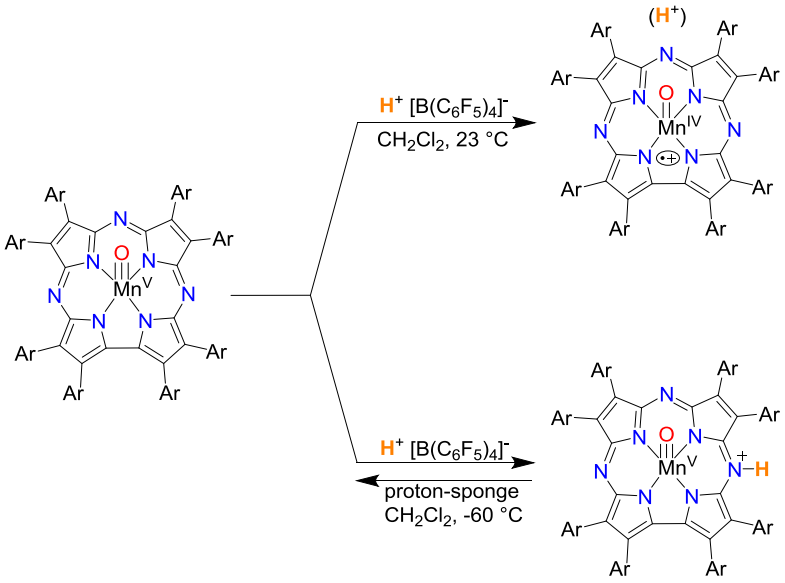

Table S1. Selected Bond Distances (Å) and Angles (deg) for $Mn^{III}(TBP_8Cz)(H_2O)$, $[Mn^{III}(H_2O)(TBP_8Cz(H))][B(C_6F_5)_4]$, and $[Mn^{III}(H_2O)(TBP_8Cz(H)_2)][B(C_6F_5)_4]_2$.

	$Mn^{III}(TBP_8Cz)(H_2O)$	$[Mn^{III}(H_2O)(TBP_8Cz(H))][B(C_6F_5)_4]$	$[Mn^{III}(H_2O)(TBP_8Cz(H)_2)][B(C_6F_5)_4]_2$
Mn(1)–N(2)	1.880(6)	1.899(4)	1.8955(19)
Mn(1)–N(4)	1.910(6)	1.899(4)	1.8944(18)
Mn(1)–N(6)	1.879(5)	1.886(4)	1.8890(18)
Mn(1)–N(7)	1.882(5)	1.901(5)	1.8897(18)
$Mn(1)–(N_{pyrrole})_{plane}$	0.377	0.359	0.332
$Mn(1)–(23–atom)_{core}$	0.566	0.604	0.526
$C_\beta–C_\beta$ (av)	1.393(5)	1.385(7)	1.391(3)
$C_\alpha–C_\beta$ (av)	1.447(5)	1.445(6)	1.442(3)
$C_\alpha–C_\alpha$ (C12–C13)	1.442(6)	1.454(6)	1.409(3)
$C_\alpha–N_{pyrrole}$ (av)	1.378(6)	1.370(6)	1.366(3)
$C_\alpha–N_{meso}$ (av)	1.344(5)	1.348(7)	1.355(3)
Mn(1)–O(1)	2.143(2)	2.116(3)	2.1152(18)
N(2)–Mn(1)–N(4)	92.2(3)	95.6(2)	92.40(8)
N(4)–Mn(1)–N(6)	89.3(2)	90.0(3)	90.14(8)
N(6)–Mn(1)–N(7)	81.1(2)	79.4(3)	79.89(8)
N(2)–Mn(1)–N(7)	88.2(3)	86.8(2)	90.50(8)
N(2)–Mn(1)–O(1)	97.7(6)	101.1(3)	102.37(8)
N(4)–Mn(1)–O(1)	101.0(6)	102.0(3)	92.33(8)
N(6)–Mn(1)–O(1)	105.0(2)	100.1(4)	98.67(8)
N(7)–Mn(1)–O(1)	102.8(4)	100.3(3)	107.42(8)

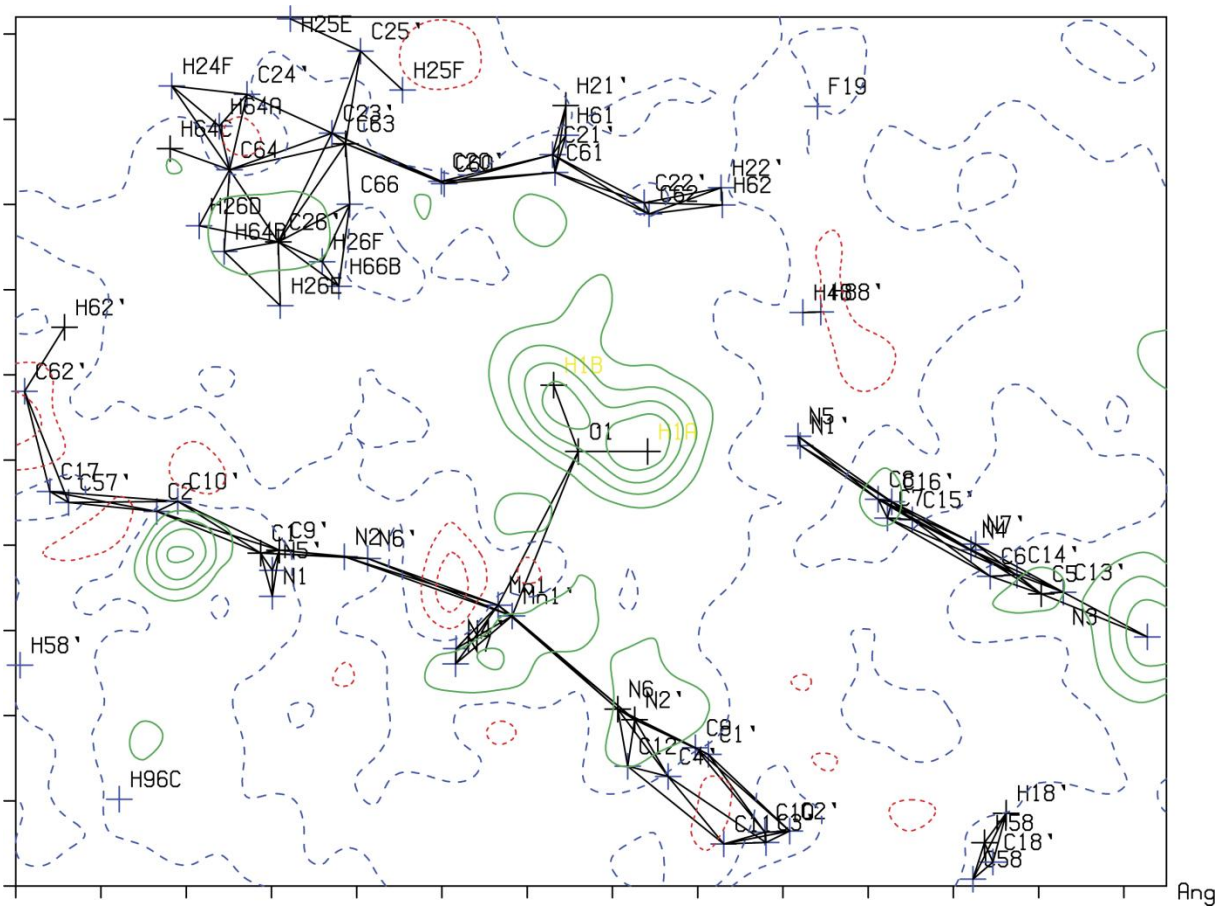

Figure S1. Contoured difference Fourier map drawn in the plane defined by O1 H1A H1B for $[Mn^{III}(H_2O)(TBP_8Cz(H))][B(C_6F_5)_4]$. The positions of the H atoms of the axial water ligand (O1) are indicated by the contoured green circles.

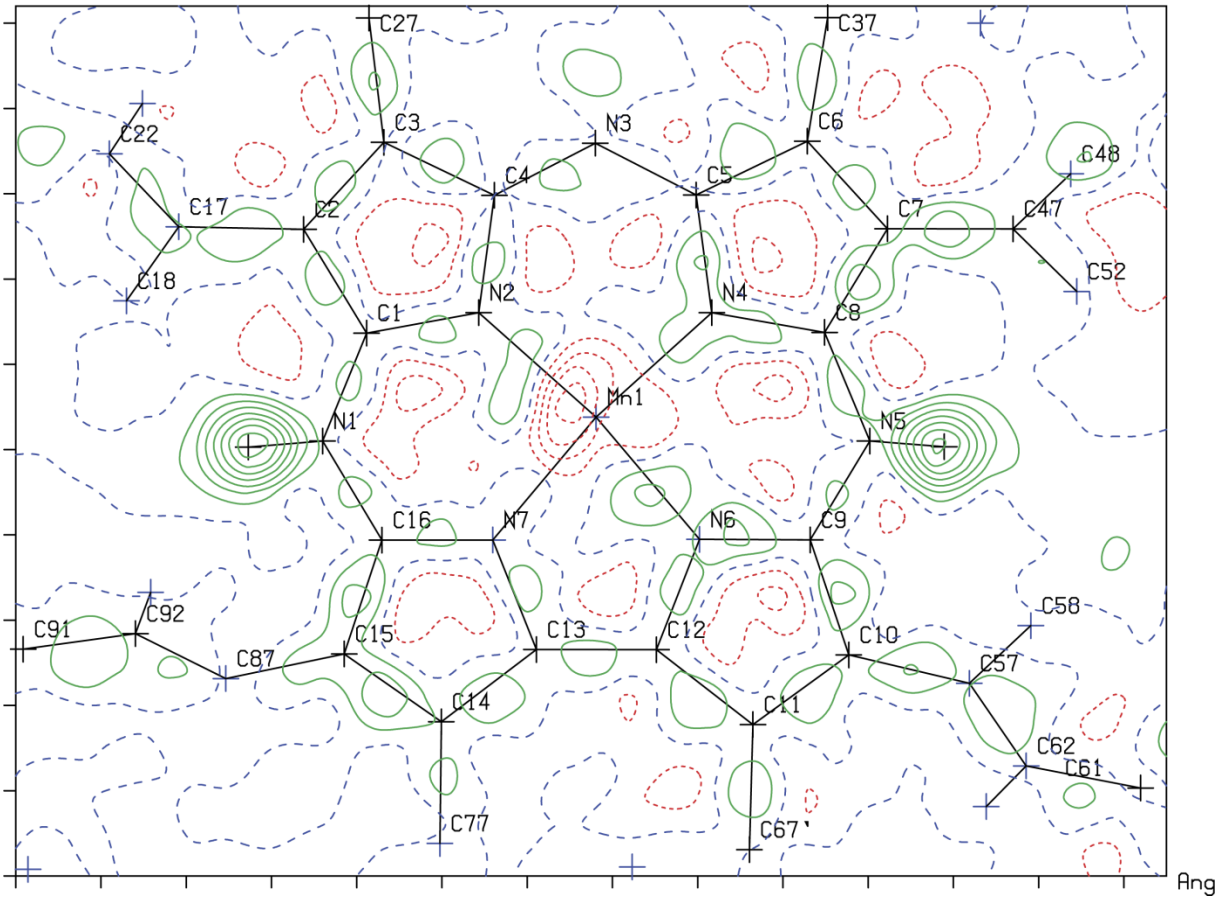

Figure S2. Contoured difference Fourier map drawn in the plane defined by N1 N3 N5 for $[Mn^{III}(H_2O)(TBP_8Cz(H)_2)][B(C_6F_5)_4]_2$. The positions of the H atoms attached to N1 and N5 are indicated by the contoured green circles.

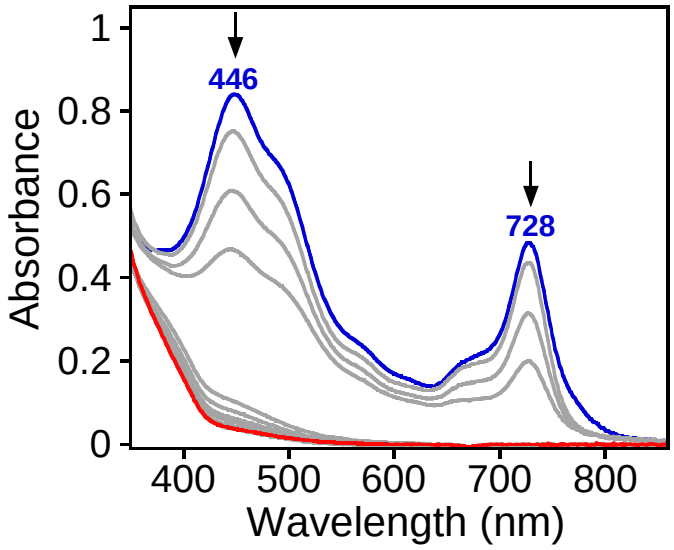

Figure S3. UV–vis spectra of the light-driven, catalytic aerobic oxidation of hexamethylbenzene (16 mM) with $Mn^{III}(TBP_8Cz)$ (16 μM) and $H^+[B(C_6F_5)_4]^-$ (32 μM) in benzene (2 mL) over 5.5 h at 23 °C.

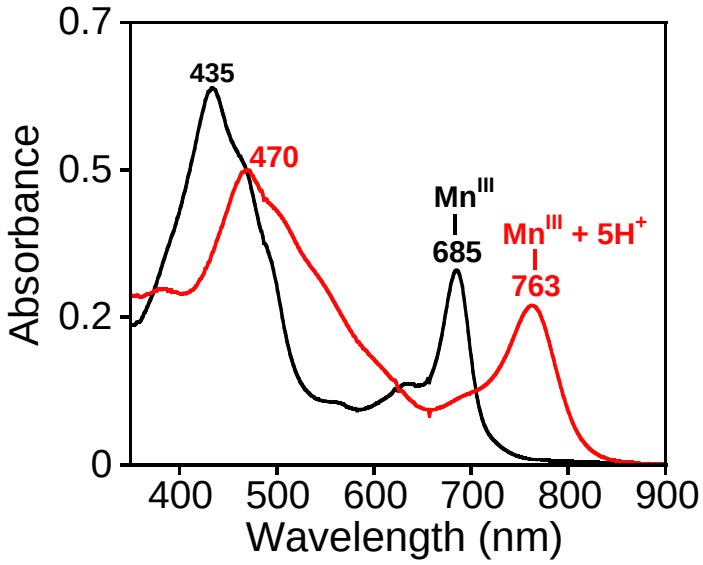

Figure S4. UV–vis spectrum of $Mn^{III}(TBP_8Cz)$ (10 μM) + $H^+[B(C_6F_5)_4]^-$ (5 equivalents) in CH_2Cl_2 (2 mL) at 23 °C.

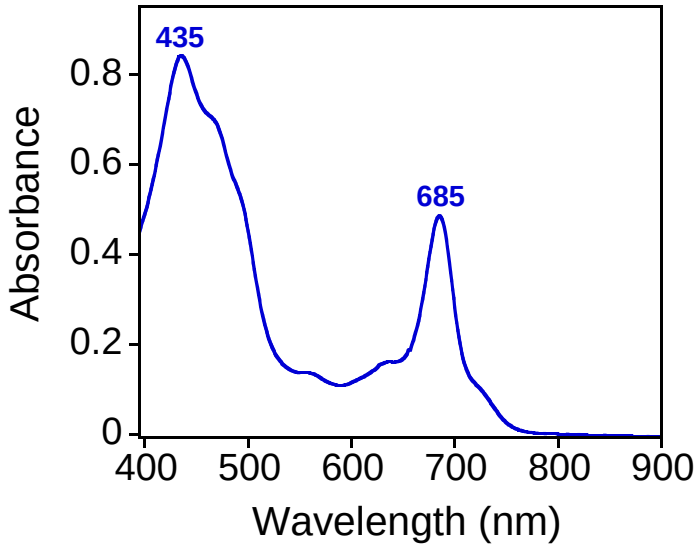

Figure S5. UV–vis spectrum of crystalline $Mn^{III}(H_2O)(TBP_8Cz)$ dissolved in CH_2Cl_2 (2 mL) at 23 °C.

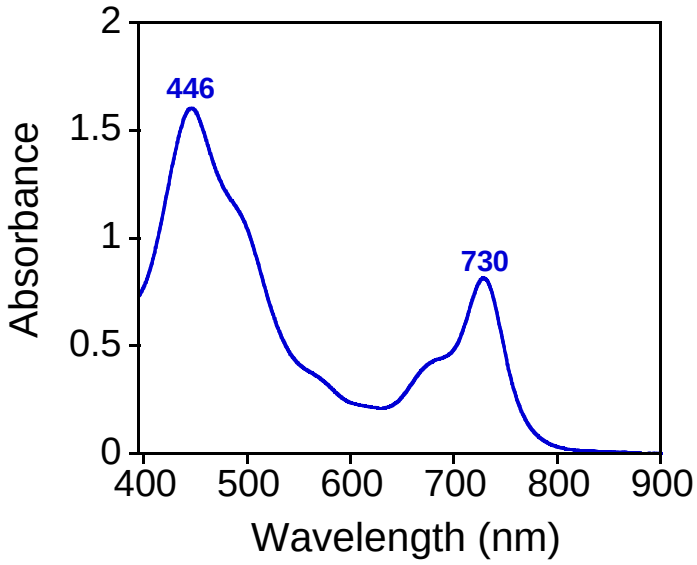

Figure S6. UV–vis spectrum of crystalline $[Mn^{III}(H_2O)(TBP_8Cz(H))][B(C_6F_5)_4]$ dissolved in CH_2Cl_2 (2 mL) at 23 °C.

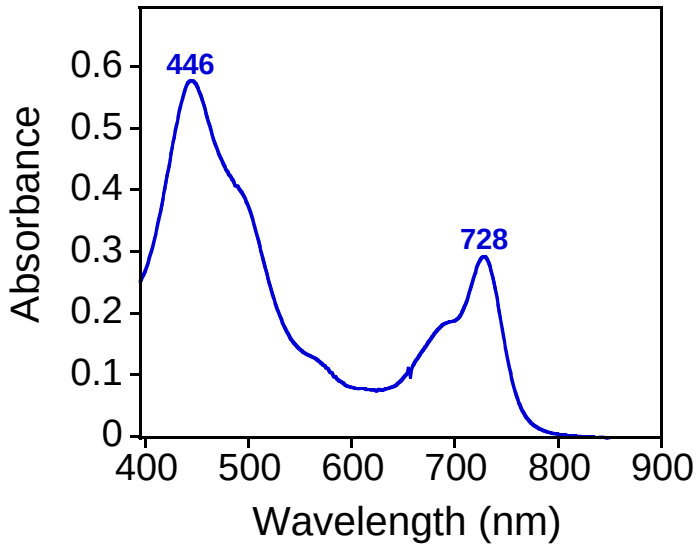

Figure S7. UV–vis spectrum of crystalline $[Mn^{III}(H_2O)(TBP_8Cz(H))][B(C_6F_5)_4]$ dissolved in HPLC grade benzene (2 mL) at 23 °C.

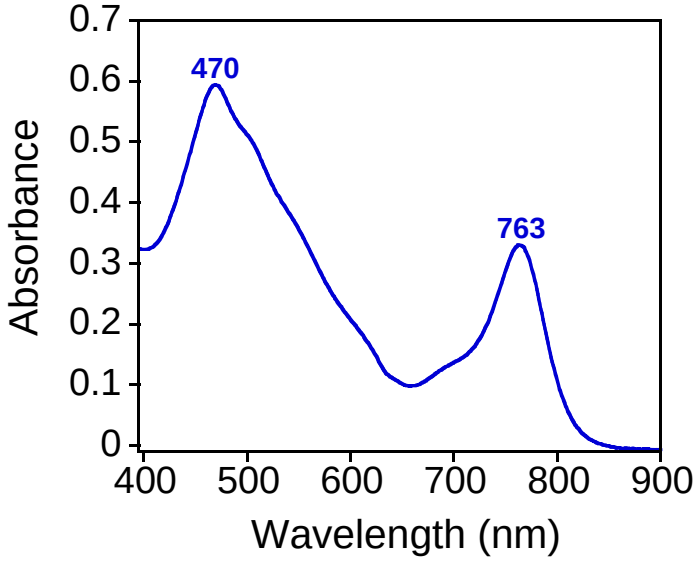

Figure S8. UV–vis spectrum of crystalline $[Mn^{III}(H_2O)(TBP_8Cz(H)_2)][B(C_6F_5)_4]_2$ dissolved in CH_2Cl_2 (2 mL) at 23 °C.

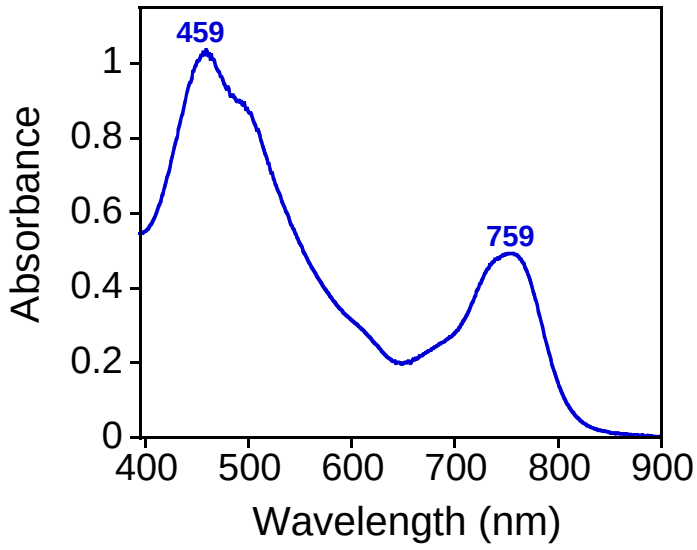

Figure S9. UV–vis spectrum of crystalline $[Mn^{III}(H_2O)(TBP_8Cz(H)_2)][B(C_6F_5)_4]_2$ (22 μM) dissolved in HPLC grade benzene (2 mL) at 23 °C.

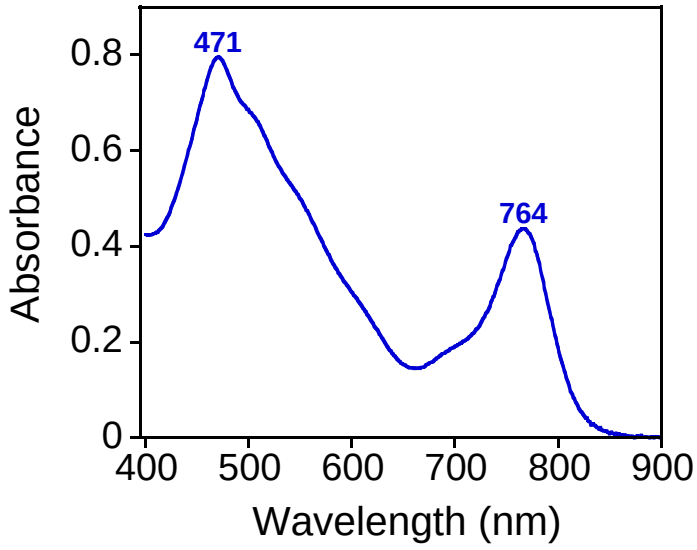

Figure S10. UV–vis spectrum following the addition of two equiv of $[H(OEt_2)_2]^+[B(C_6F_5)_4]^-$ (30 μM) to $Mn^{III}(H_2O)(TBP_8Cz)$ (15 μM) dissolved in dry, doubly–distilled benzene (3 mL) under N_2 at 23 °C.

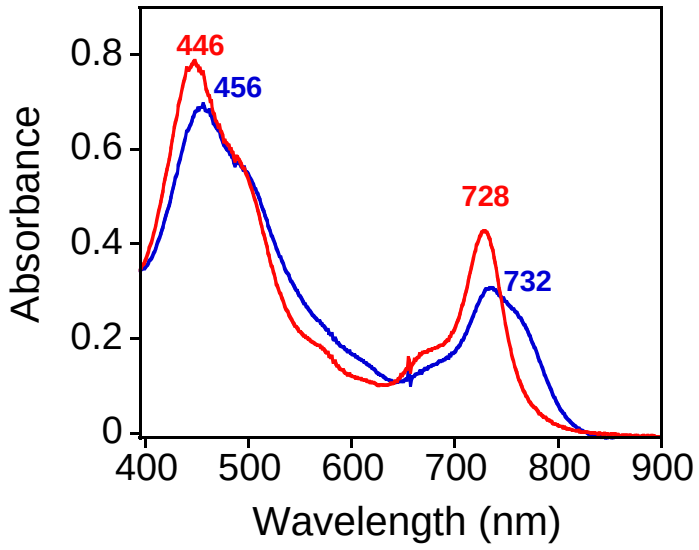

Figure S11. (blue line) UV–vis spectrum following the addition of two equiv of $[H(OEt_2)_2]^+[B(C_6F_5)_4]^-$ (28 μM) to $Mn^{III}(H_2O)(TBP_8Cz)$ (14 μM) dissolved in HPLC grade benzene (3 mL) at 23 °C. (red line) UV–vis spectrum following the addition of water (10 μL) to the solution.

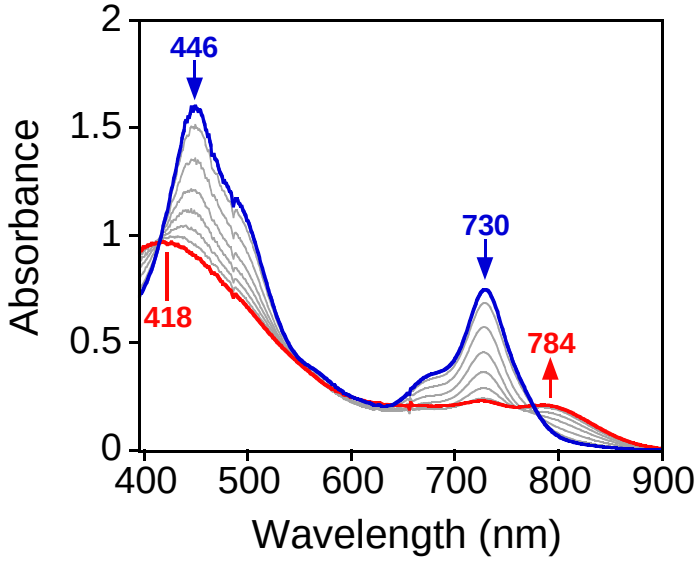

Figure S12. UV–vis spectra of the photoirradiation under aerobic conditions of a solution of $[Mn^{III}(H_2O)(TBP_8Cz(H))][B(C_6F_5)_4]$ (22 μM) and HMB (22 mM) (blue line) to give $[Mn^{IV}(O)(TBP_8Cz^{\bullet+})(H)]^+$ (red line) in CH_2Cl_2 (2 mL) over 15 min at 23 °C.

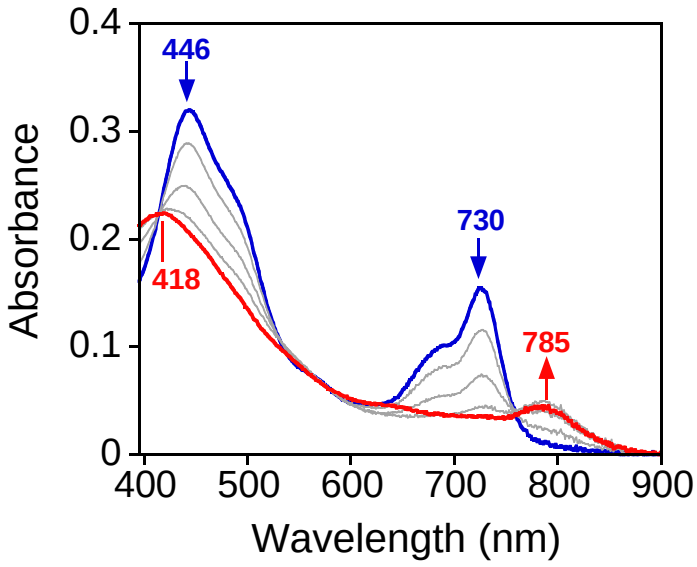

Figure S13. UV–vis spectra of $[Mn^{III}(H_2O)(TBP_8Cz(H))][B(C_6F_5)_4]$ (5 μM) + excess PhIO (blue line) to give $[Mn^{IV}(O)(TBP_8Cz^{\bullet+})(H)]^+$ (red line) in CH_2Cl_2 (3 mL) over 5 min at 23 °C.

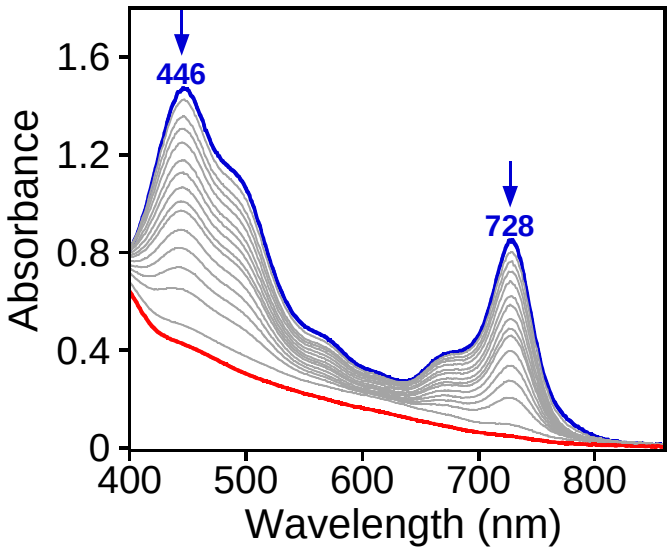

Figure S14. UV–vis spectra of the light-driven, catalytic aerobic oxidation of hexamethylbenzene (27 mM) with $[Mn^{III}(H_2O)(TBP_8Cz(H)_2)][B(C_6F_5)_4]_2$ (27 μM) in benzene (3 mL) over 5 h at 23 °C.

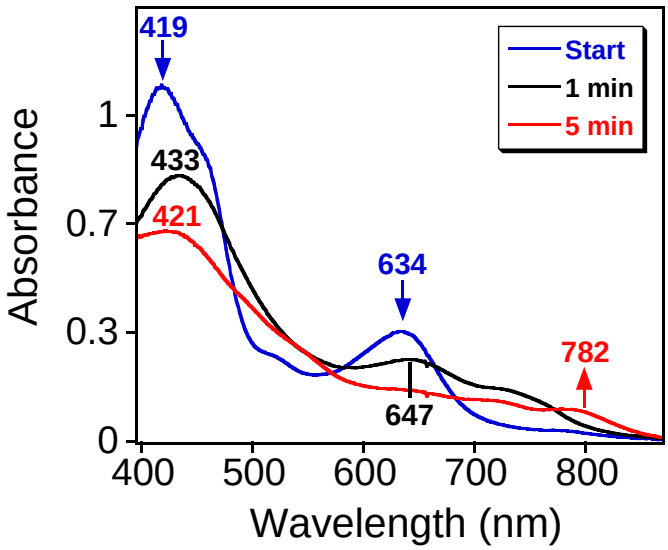

Figure S15. UV–vis spectra of $Mn^{V}(O)(TBP_8Cz)$ (17 μM) + $H^{+}[B(C_6F_5)_4]^{-}$ (17 μM) (blue line) to give $[Mn^{IV}(O)(TBP_8Cz^{\bullet+})(H)]^{+}$ (red line) in CH_2Cl_2 (3 mL) over 5 min at 23 °C.

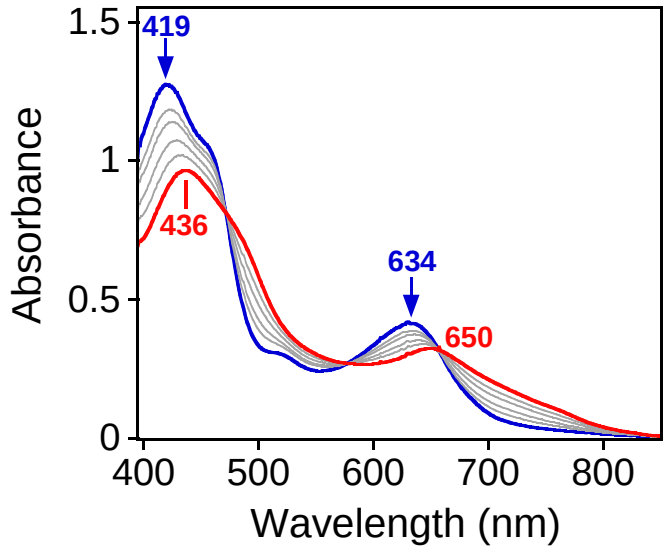

Figure S16. UV−vis spectral changes (0 – 1 min) for the addition of $H^{+}[B(C_6F_5)_4]^{-}$ (19 μM) to $Mn^{V}(O)(TBP_8Cz)$ (19 μM) (blue line) to give $[Mn^{V}(O)(TBP_8Cz(H))]^{+}$ (red line) in CH_2Cl_2 (3 mL) at –60 °C .

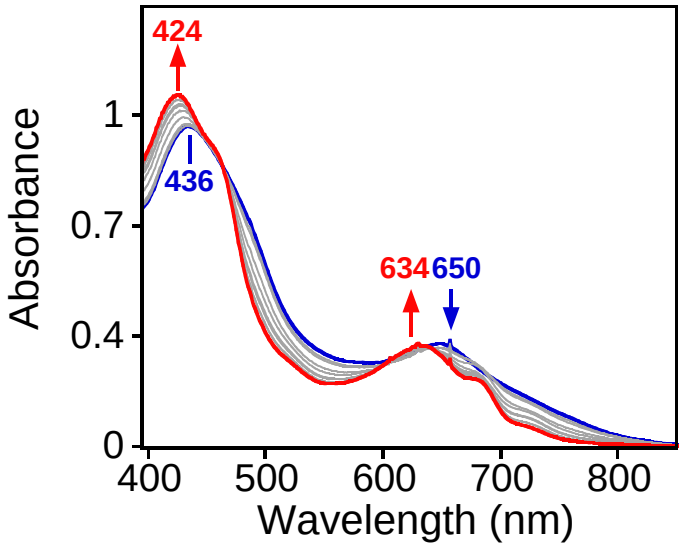

Figure S17. UV–vis spectra for the addition of proton sponge (19 μM) to $[Mn^{V}(O)(H)(TBP_8Cz)]^{+}$ (19 μM) (blue line) to give $Mn^{V}(O)(TBP_8Cz)$ (red line) in CH_2Cl_2 (3 mL) at –60 °C.

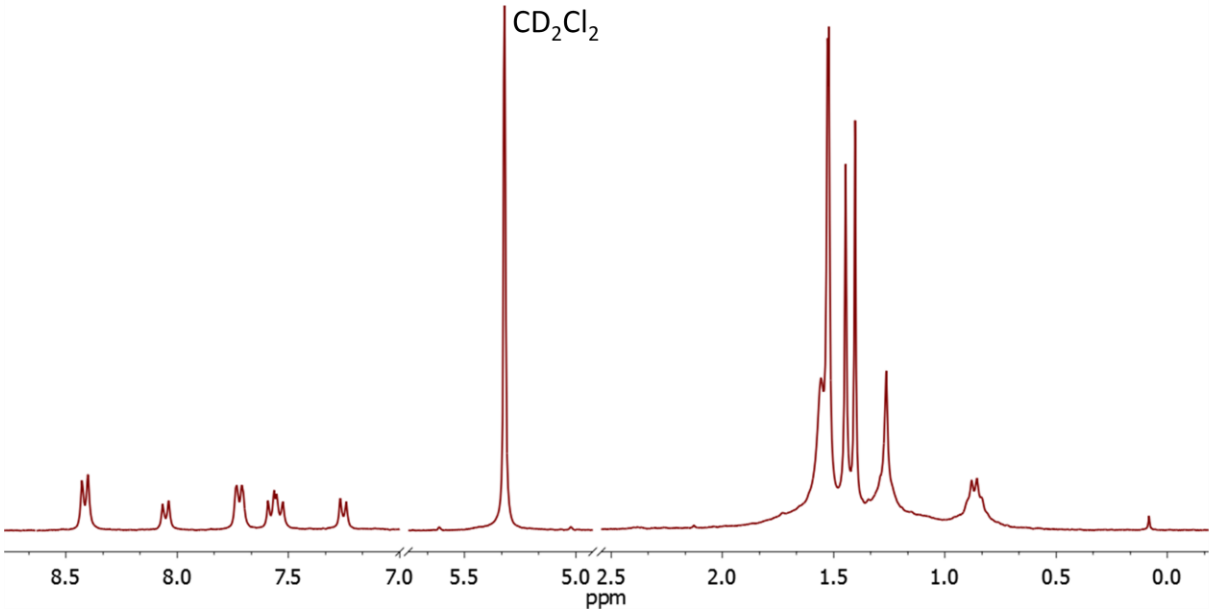

Figure S18. ^{1}H–NMR of $Mn^{V}(O)(TBP_8Cz)$ (1.4 mM) in CD_2Cl_2 at 24 °C.

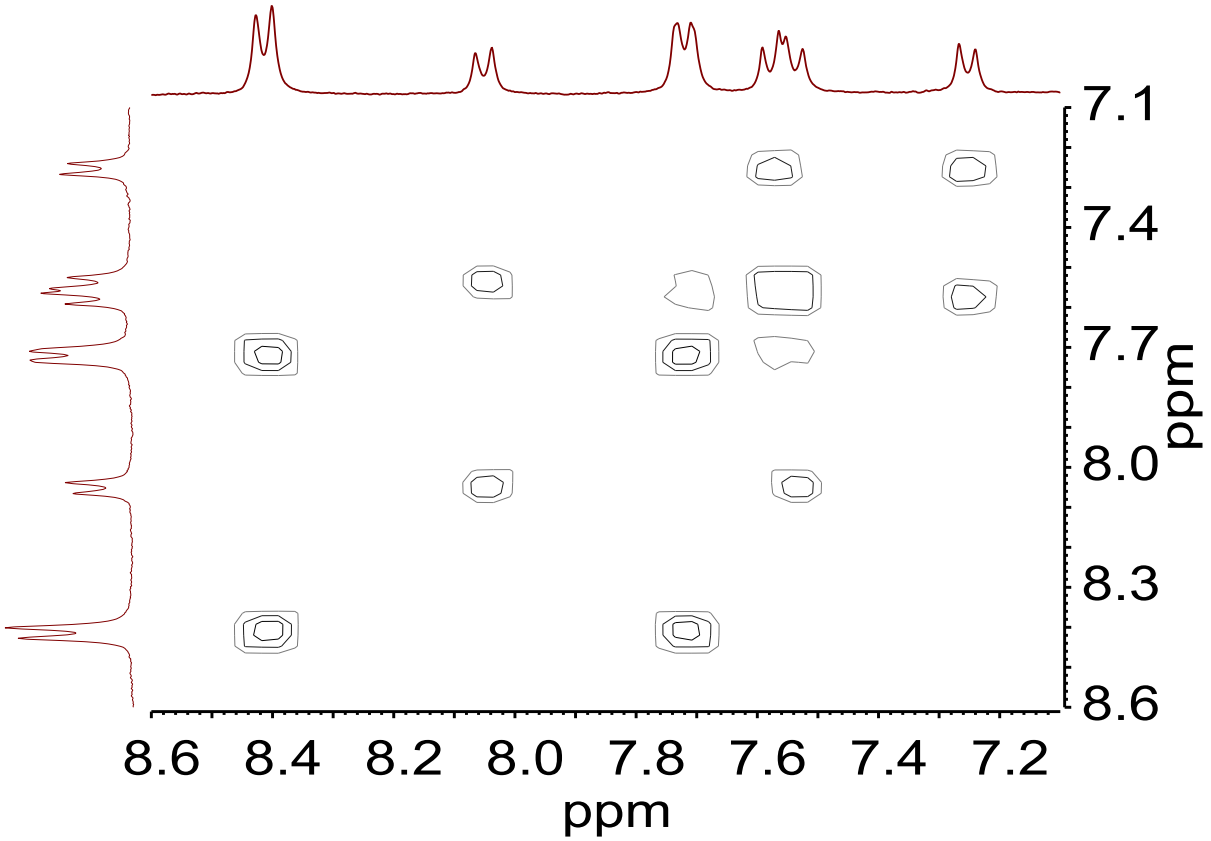

Figure S19. $^{1}H–^{1}H$ 2D COSY spectrum of $Mn^{V}(O)(TBP_8Cz)$ (1.4 mM) in CD_2Cl_2 at 24 °C (aromatic region).

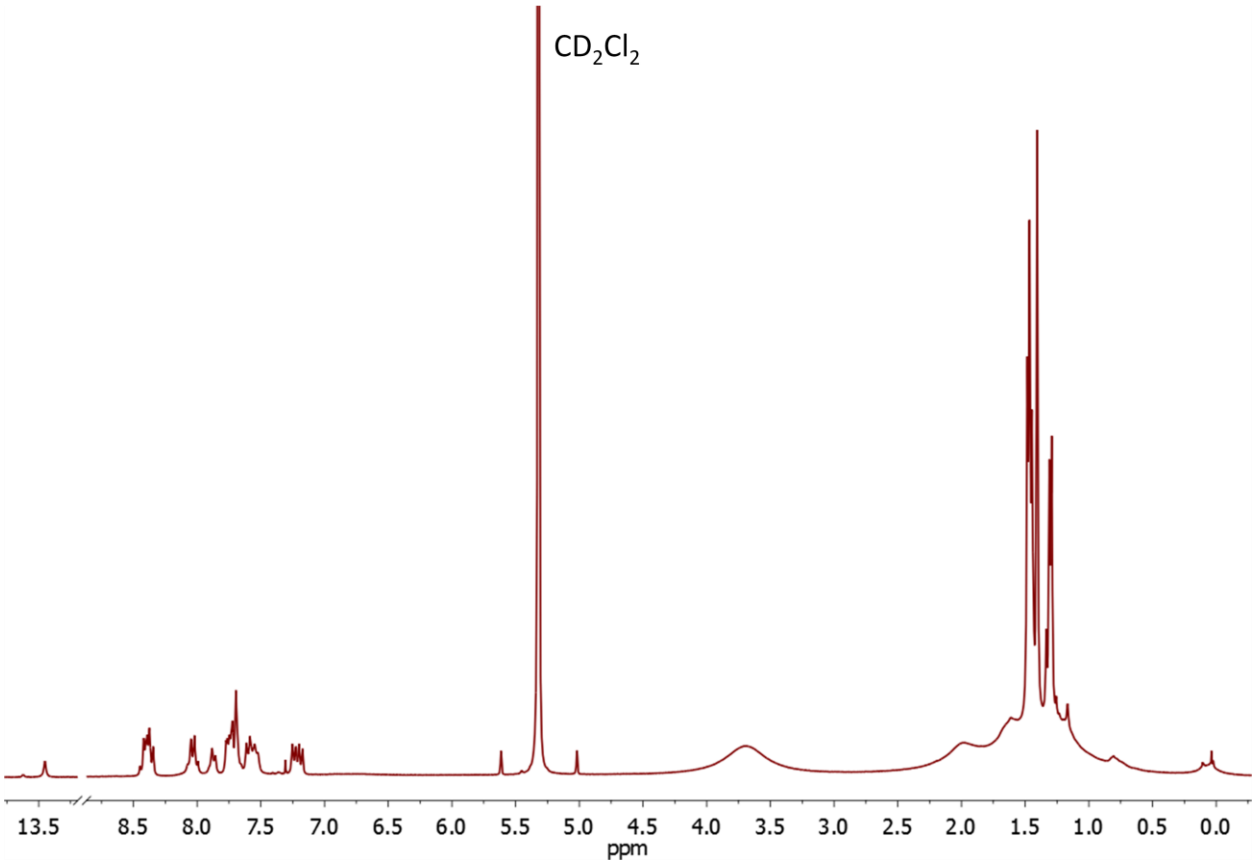

Figure S20. ^{1}H–NMR of $[Mn^{V}(O)(TBP_8Cz(H))]^{+}$ (1 mM) in CD_2Cl_2 at –60 °C.

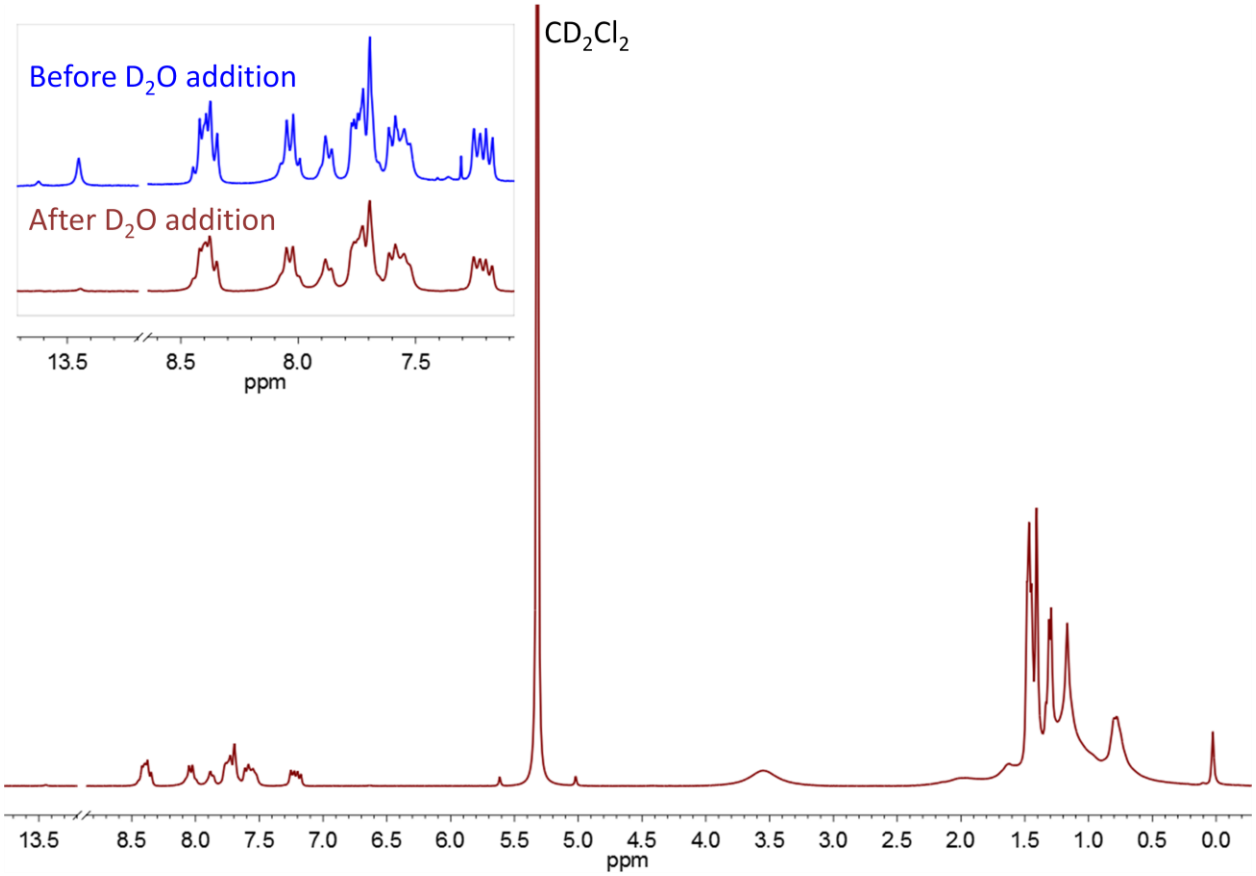

Figure S21. ^{1}H–NMR of $[Mn^V(O)(TBP_8Cz(H))]^+$ (1.4 mM) with added D_2O (63 mM) in CD_2Cl_2 at –60 °C. Insert: $[Mn^V(O)(TBP_8Cz(H))]^+$ ^{1}H–NMR spectrum (7.1–13.7 ppm) before addition of D_2O (blue) and after addition of D_2O (red).

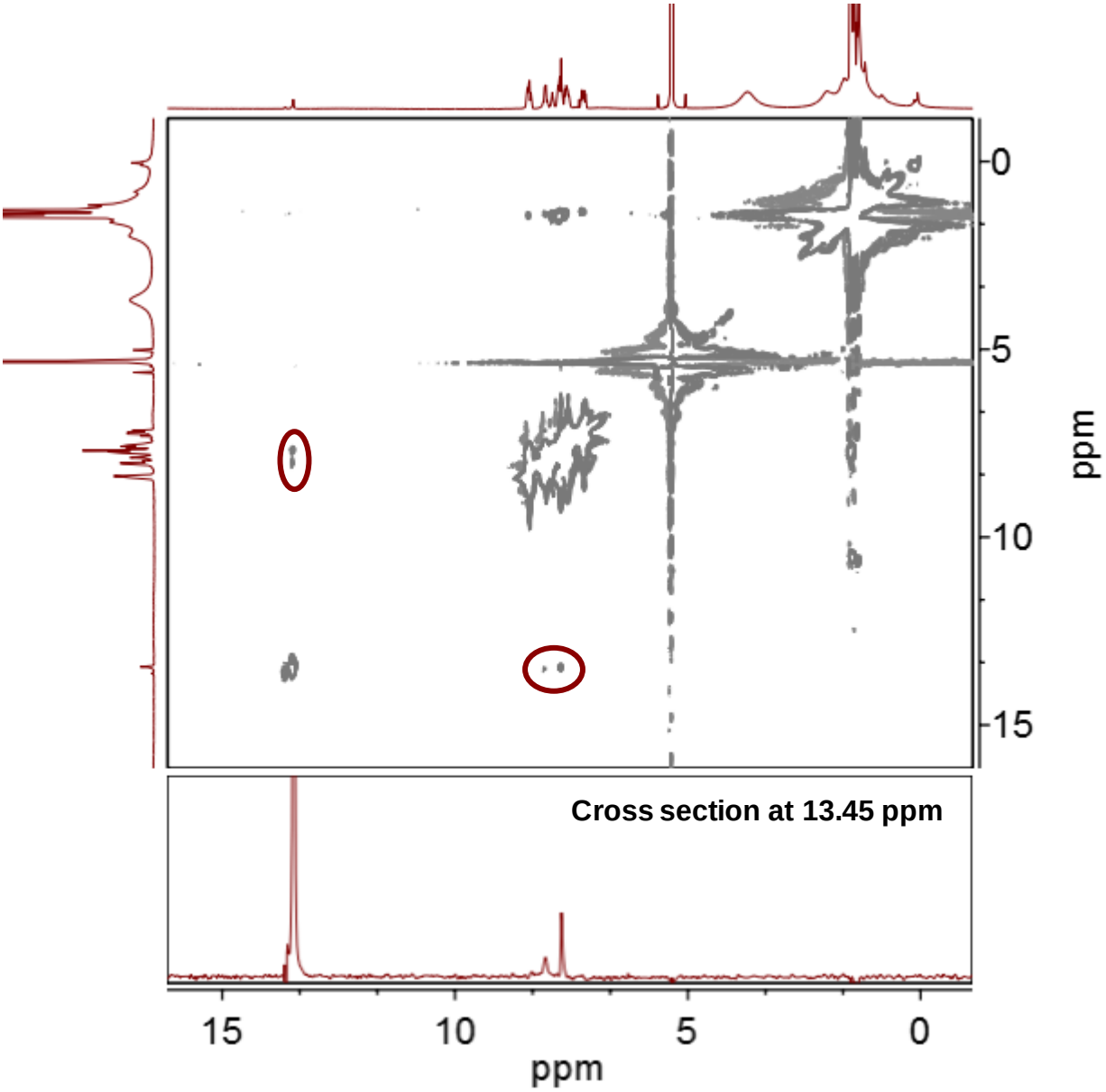

Figure S22. $^{1}H–^{1}H$ 2D NOESY spectrum of $[Mn^{V}(O)(TBP_8Cz(H))]^{+}$ (3.9 mM) in CD_2Cl_2 at –60 °C. Relevant through–space interactions are highlighted. Cross section at 13.45 ppm displayed on bottom.

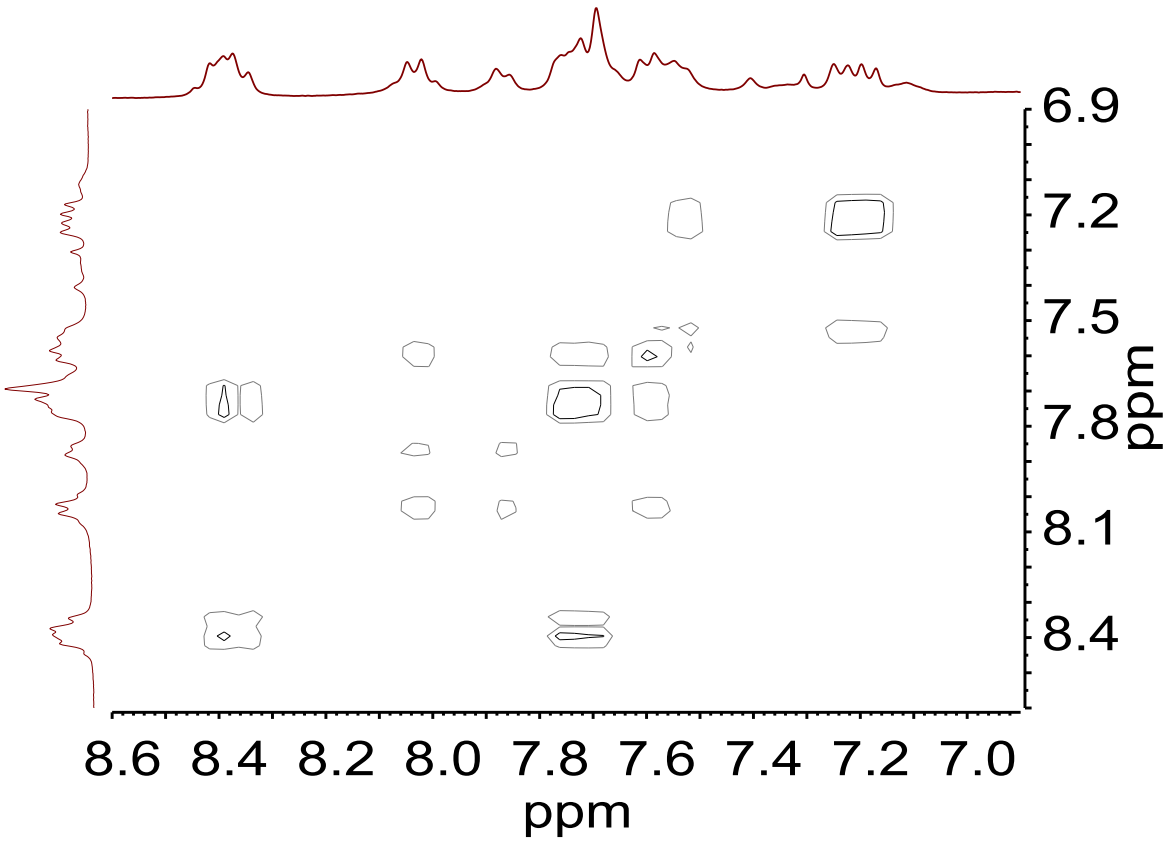

Figure S23. ^{1}H–^{1}H 2D COSY spectrum of $[Mn^{V}(O)(TBP_8Cz(H))]^{+}$ (3.9 mM) in CD_2Cl_2 at –60 °C (aromatic region).